Cusped rainbows and incoherence effects in the rippling-mirror model for particle scattering from surfaces

1975 J. Phys. A: Math. Gen. 8 566

(http://iopscience.iop.org/0305-4470/8/4/019)

J. Phys. A: Math. Gen., Vol. 8, No. 4, 1975. Printed in Great Britain.

Cusped rainbows and incoherence effects in the rippling-mirror model for particle scattering from surfaces

M V Berry

H H Wills Physics Laboratory, Bristol University, Tyndall Avenue, Bristol BS8 1TL, UK

Received 9 September 1974

Abstract. We consider scattering from a corrugated hard surface Σ with random moving perturbations (a 'rippling mirror'). Kirchhoff's approximation enables the classical limit, diffraction effects and incoherence to be treated within the same framework. The classical rainbow is a curve $\mathscr{C}$ in the two-dimensional space of deflections G; we study the topology of $\mathscr{C}$ and show that it has cusps whose positions are sensitive to the form of Σ. Classically the scattering is singular on Σ but diffraction softens the singularities; we give the diffraction functions to be used near and on smooth parts and cusps of $\mathscr{C}$, and derive criteria for the observability of rainbow structure (taking account of surface periodicity which quantizes G). Random thermal perturbations of Σ blur the diffracted beams; we introduce a simple approximation for the blurring function, and this suggests a simple method for inverting experimental data to obtain the 'surface phonon spectrum', even in cases where 'multiphonon processes' dominate.

1. Introduction

The scattering of beams of particles (atoms, molecules or ions) from solid surfaces can give useful information about particle–solid interactions (Toennies 1974). To extract this information from the experimental results, however, one requires a workable theory, that is a theory that is neither so simple that it fails to describe a wide range of phenomena nor so complicated that detailed predictions cannot easily be made. From this point of view the most useful theory so far assumes that the interaction potential between particle and solid is zero outside a surface Σ, and rises suddenly to infinity as the particle approaches the solid through Σ. This totally reflecting surface has predominantly the two-dimensional periodicity of the surface of a perfect solid, but is perturbed in a random manner by thermal effects. To describe approximately the scattering from this 'rippling mirror' the theory employs Kirchhoff's diffraction integral, rather than giving an exact treatment based on the wave equation. We use the expression 'rippling mirror' instead of the more common 'corrugated hard surface' because we wish explicitly to consider the inelastic effects of the time dependence of the random perturbations of Σ.

The exact quantum scattering from the rippling mirror Σ has been discussed in detail by Beeby (1972, 1973), while the additional Kirchhoff approximation has been used by Garibaldi *et al* (1974), who call it the eikonal approximation. Using a special form for Σ, these latter authors give a quantum-mechanical analysis of the classical surface rainbow discovered by McClure (1970) and Smith *et al* (1969). They also give a

formalism for the inelastic and diffuse incoherent scattering that arises from the space-and-time-dependent parts of the random perturbation of Σ, but they do not discuss the nature of this incoherent scattering.

In this paper we use exactly the same scattering model as Garibaldi *et al* (1974), but we go further, and obtain some rather simple general results. The first concerns rainbows: by examining more realistic surfaces Σ, which are less symmetrical than that of Garibaldi *et al*, we establish the topology of the classical rainbow in the image domain, that is, in the two-dimensional space of directions of the scattered particles. In this space the rainbow consists of two closed curves ('caustics'), one inside the other; the inner curve has several cusps (the number depends on the symmetry of the lattice). Our second result concerns the diffraction functions that must be used to describe the quantum-mechanical softening of the classical rainbow singularities near smooth and cusped caustics. We discuss the conditions under which these phenomena could be observed. Our final result concerns incoherent scattering: we derive a simple approximate formula, of apparently rather general applicability, giving the diffuse and inelastic incoherent scattering *explicitly* in terms of the spectrum of the random perturbations of Σ; the formula gives a very simple method, in principle, of determining this spectrum from scattering data, and may solve a puzzle concerning 'multiphonon processes' (Beeby 1973).

Before beginning our main argument we discuss briefly the limitations of the model used. By approximating the actual smooth particle–solid potential by the (repulsive) hard mirror Σ, we are neglecting the effects of the attractive potential well beyond the hard core. The principal such effects are a modification of the incident-beam wavevector near the mirror (Beeby 1971, Garibaldi *et al* 1974), and the existence of surface bound states into which the incident particles may fall (Lennard-Jones and Devonshire 1937, Cabrera *et al* 1970, Wolken 1973). By employing Kirchhoff diffraction theory, we are neglecting multiple reflections between different parts of the surface (Beeby 1972, Beckmann and Spizzichino 1963). Such reflections will be insignificant if the total variation $\Delta\theta$ of surface slopes is small and if the incident beam does not graze the surface; in fact $\Delta\theta$ does not exceed about 10° (Nahr, private communication), so that the use of Kirchhoff's integral should not involve any serious approximation. In addition, our scattering model implicitly neglects recoil effects, that is, any influence of the projectiles on the solid; this will be justified if the projectiles are light and the solid atoms heavy and tightly bound.

2. Kirchhoff diffraction theory

We employ Cartesian coordinates $\boldsymbol{r} = (x, y, z)$ to locate points in space. In the 'horizontal' plane $z = 0$ we locate points by $\boldsymbol{R} = (x, y)$. The form of the rippling mirror Σ at time t is defined by its height $h(\boldsymbol{R}, t)$ above the plane $\boldsymbol{R}$. The function h is the sum of a periodic stationary part $h_p(\boldsymbol{R})$ and a time-dependent random perturbation $h_r(\boldsymbol{R}, t)$, ie

$$h(\boldsymbol{R}, t) = h_p(\boldsymbol{R}) + h_r(\boldsymbol{R}, t), \tag{2.1}$$

where

$$h_p(\boldsymbol{R} + m\boldsymbol{a} + n\boldsymbol{b}) = h_p(\boldsymbol{R}), \tag{2.2}$$

$\boldsymbol{a}$ and $\boldsymbol{b}$ being unit vectors in the surface lattice and m and n being integers.

The incident beam is represented quantum-mechanically by a single plane wave $\psi_{inc}(\boldsymbol{r}, t)$ with frequency ω_0 (corresponding to an energy $E_0 = \hbar\omega_0$) and wavevector $\boldsymbol{k}_0$.

The wavelength is $\lambda_0 = 2\pi/k_0 = h/(2mE_0)^{1/2}$, where m is the mass of the particles. The horizontal component of $\boldsymbol{k}_0$ is $\boldsymbol{K}_0$ and the vertical component k_{0z} is negative because the wave is approaching Σ from above. Obviously $K_0 < k_0$ for physically interesting waves. The scattered particles emerge in different directions $\boldsymbol{k}$ and with different frequencies ω (because of the Doppler shifts caused by the time dependence of h_r); therefore we represent them by a wavefunction $\psi_{sc}(\boldsymbol{r}, t)$ which is a sheaf of plane waves receding from Σ, so that the vertical component k_z of $\boldsymbol{k}$ is positive if the magnitude K of the horizontal component $\boldsymbol{K}$ is less than k, and positive imaginary (corresponding to evanescent waves) if $K > k$. Thus we can write ψ_{inc} and ψ_{sc} in the form

$$\psi_{inc}(\boldsymbol{r}, t) = \exp[\mathrm{i}(\boldsymbol{K}\cdot\boldsymbol{R} - |k_{0z}|z - \omega_0 t)]$$

$$\psi_{sc}(\boldsymbol{r}, t) = \iint \mathrm{d}\boldsymbol{K} \int_{-\infty}^{\infty} \mathrm{d}\omega a(\boldsymbol{K}_0, \omega_0; \boldsymbol{K}, \omega) \exp[\mathrm{i}(\boldsymbol{K}\cdot\boldsymbol{R} + k_z z - \omega t)], \qquad (2.3)$$

where a is the amplitude of the wave specified by $\boldsymbol{K}$ and ω (we could specify each wave by its three-dimensional wavevector $\boldsymbol{k}$, but the form written is more useful).

We wish to calculate the amplitudes a. This we do by using the boundary condition that the total wave $\psi_{inc} + \psi_{sc}$ vanishes on Σ. Strictly speaking the form (2.3) for ψ_{sc} is exact only if z exceeds the largest value of $h(\boldsymbol{R}, t)$; for smaller z (but still above Σ) there will be small-amplitude waves that have been scattered from the hills down into the valleys of Σ. This effect will cause multiple scattering, and we neglect it. Thus the boundary condition on Σ gives the following integral equation for a:

$$\exp[\mathrm{i}(\boldsymbol{K}_0\cdot\boldsymbol{R} - |k_{0z}|h(\boldsymbol{R}, t) - \omega_0 t)]$$

$$= -\iint \mathrm{d}\boldsymbol{K} \int_{-\infty}^{\infty} \mathrm{d}\omega a(\boldsymbol{K}_0, \omega_0; \boldsymbol{K}, \omega) \exp[\mathrm{i}(\boldsymbol{K}\cdot\boldsymbol{R} + k_z h(\boldsymbol{R}, t) - \omega t)]. \qquad (2.4)$$

This holds for all $\boldsymbol{R}$ and t. Unfortunately this equation cannot be solved exactly for a in closed form. But we notice that if h is zero or varies linearly with $\boldsymbol{R}$ and t we can use Fourier's theorem, to obtain

$$a(\boldsymbol{K}_0, \omega_0; \boldsymbol{K}, \omega)$$

$$= \frac{-1}{(2\pi)^3} \iint \mathrm{d}\boldsymbol{R} \int \mathrm{d}t \exp\{\mathrm{i}[(\boldsymbol{K}_0 - \boldsymbol{K})\cdot\boldsymbol{R} - (|k_{0z}| + k_z)h(\boldsymbol{R}, t) - (\omega_0 - \omega)t]\}. \qquad (2.5)$$

This is exact if

$$h(\boldsymbol{R}, t) = \boldsymbol{P}\cdot\boldsymbol{R} + vt \qquad (2.6)$$

which corresponds to a flat surface inclined at an angle $\tan^{-1}|\boldsymbol{P}|$ (to the horizontal), whose contours are perpendicular to $\boldsymbol{P}$ and which moves upwards at the constant speed v. Then (2.5) gives

$$a(\boldsymbol{K}_0, \omega_0; \boldsymbol{K}, \omega) = -\delta(\boldsymbol{K}_0 - \boldsymbol{K} + (|k_{0z}| + k_z)\boldsymbol{P})\delta(\omega - \omega_0 - (|k_{0z}| + k_z)v). \qquad (2.7)$$

It can be verified that this correctly describes specular reflection from $\boldsymbol{K}_0$ into a direction $\boldsymbol{K}$ determined by the slope $\boldsymbol{P}$ of Σ, with the frequency Doppler shifted from ω_0 to ω by the motion of Σ.

Kirchhoff diffraction theory consists in using (2.5) for general surfaces Σ, which do not have the simple form (2.6). This will obviously be a better approximation, the smaller are the curvatures and accelerations of Σ. The principal advantage of (2.5) is the variety of phenomena it can describe. It is the simplest expression describing scattering from

surfaces whose deviations from flatness may range from small perturbations to hills and dales many wavelengths in extent, for which classical mechanics gives a good description for the reflection (see § 3). This is particularly useful in particle–surface scattering, because it is often the case that reflection of h_p (cf (2.1)) may be treated classically or semiclassically while h_r is so small that its effects must be calculated using diffraction theory. Another property of (2.5) is that it gives at least a first approximation to the evanescent waves, for which $K > k$.

Experimentally, what is measured is the current of particles (far from the surface) travelling in a small range of directions about a chosen direction $\boldsymbol{K}$ with energies lying within a small range about a chosen energy $\hbar\omega$. If the surface is infinite in extent, or the experiment infinite in duration, then this current will be infinite; therefore we calculate the current I per unit area of Σ per unit time. If Σ has a (large) illuminated area $\mathscr{A}$ and the experiment lasts for a (long) time $\mathscr{T}$, then the current is proportional to

$$I(\boldsymbol{K}_0, \omega_0; \boldsymbol{K}, \omega) = \frac{|a(\boldsymbol{K}_0, \omega_0; \boldsymbol{K}, \omega)|^2 (2\pi)^3}{\mathscr{A}\mathscr{T}}, \tag{2.8}$$

apart from purely kinematic factors (for a discussion of these, see Garibaldi *et al* 1974). We shall find that this expression always gives sensible results. For example, in the case of the flat surface (2.6), $|a|^2$ would involve squares of delta functions (see (2.7)). These simplify as follows: we write, symbolically,

$$\begin{aligned}\delta^2(\boldsymbol{K})\delta^2(\omega) &= \delta(\boldsymbol{K})\delta(\omega) \lim_{\mathscr{A}\mathscr{T}\to\infty} \left(\frac{1}{(2\pi)^2} \iint_{\mathscr{A}} \mathrm{d}\boldsymbol{R}\, \mathrm{e}^{\mathrm{i}\boldsymbol{K}\cdot\boldsymbol{R}} \times \frac{1}{2\pi} \int_{\mathscr{T}} \mathrm{d}t\, \mathrm{e}^{\mathrm{i}\omega t} \right) \\ &= \delta(\boldsymbol{K})\delta(\omega)\mathscr{A}\mathscr{T}/(2\pi)^3. \end{aligned} \tag{2.9}$$

Thus (2.8) gives, for this case,

$$I = \delta(\boldsymbol{K} - \boldsymbol{K}_0 + (|k_{0z}| + k_z)\boldsymbol{P})\delta(\omega_0 - \omega - (|k_{0z}| + k_z)v), \tag{2.10}$$

an expression corresponding to a finite total intensity.

3. Perfect periodicity: topology of classical rainbows

If Σ is periodic, that is, if we are ignoring the effects of thermal disturbances, we can set h_r in (2.1) equal to zero, and expand in a Fourier series the function of $h_p(\boldsymbol{R})$ that appears in the diffraction integral (2.5). Then, using (2.8), the intensity I becomes

$$I(\boldsymbol{K}_0, \omega_0; \boldsymbol{K}, \omega) = \delta(\omega - \omega_0) \sum_{\boldsymbol{G}} |S_{\boldsymbol{G}}|^2 \delta(\boldsymbol{K} - \boldsymbol{K}_0 - \boldsymbol{G}). \tag{3.1}$$

We have reproduced here the well known result that in this case the scattering is elastic ($\omega = \omega_0$), and the emergent particles appear as a series of *diffracted beams* in directions $\boldsymbol{K} = \boldsymbol{K}_0 + \boldsymbol{G}$, where $\boldsymbol{G}$ are the two-dimensional vectors of the reciprocal surface lattice. The strength of the $\boldsymbol{G}$th diffracted beam is $|S_{\boldsymbol{G}}|^2$, where the diffraction amplitude $S_{\boldsymbol{G}}$ is given by

$$S_{\boldsymbol{G}} = \frac{1}{A} \iint_{\text{unit cell}} \mathrm{d}\boldsymbol{R} \exp\{-\mathrm{i}[\boldsymbol{G} \cdot \boldsymbol{R} + (|k_{0z}| + k_z)h_p(\boldsymbol{R})]\}. \tag{3.2}$$

(A is the area of the unit cell.)

The hemisphere of directions of scattered particles corresponds to the circle $|\boldsymbol{K}| < k_0$ in the 'image' plane $\boldsymbol{K}$. This circle has area πk_0^2. Each diffracted beam 'occupies' a unit reciprocal lattice cell in $\boldsymbol{K}$ space. Each such cell has area $4\pi^2/A$. Thus the number $\mathcal{N}$ of observed diffracted beams is

$$\mathcal{N} = \frac{Ak_0^2}{4\pi} = \frac{\pi A}{\lambda_0^2} = \frac{mAE_0}{2\pi\hbar^2}. \tag{3.3}$$

Now, under nearly classical conditions we may regard λ_0 and $\hbar$ as small, or m and k_0 as large. Thus $\mathcal{N}$ is large, the diffracted beams are densely distributed in direction, and the 'deflection' $\boldsymbol{G} = \boldsymbol{K} - \boldsymbol{K}_0$ in (3.2) may be regarded as a quasi-continuous variable. We wish to discuss the form of $S_{\boldsymbol{G}}$ under these *semiclassical* conditions.

The important point is that when $k_0 (= k)$ is large the integrand of (3.2) oscillates rapidly as $\boldsymbol{R}$ traverses the unit cell, and most of the area of integration gives no contribution, because of destructive interference. However at isolated points $\boldsymbol{R}_i(\boldsymbol{K}_0, \boldsymbol{G})$ where the *phase of the integrand is stationary* this cancellation does not occur, and we obtain contributions to $S_{\boldsymbol{G}}$. The stationary points $\boldsymbol{R}_i$ are given by

$$\boldsymbol{G} = -(|k_{0z}| + k_z)\nabla h_p(\boldsymbol{R}_i). \tag{3.4}$$

But this is exactly the condition for a surface point $\boldsymbol{R}$ to reflect a classical particle specularly from $\boldsymbol{K}_0$ to $\boldsymbol{K}_0 + \boldsymbol{G}$, so that we have found that only the classical paths contribute to the quantum diffraction integral (3.2) when k_0 is large. In interpreting all our subsequent classical and semiclassical formulae, it should not be forgotten that (3.4) is really an implicit equation for $\boldsymbol{G}$, since this vector appears also in

$$k_z (= [k^2 - (\boldsymbol{K}_0 + \boldsymbol{G})^2]^{1/2});$$

for gently-varying surfaces Σ this dependence of k_z on $\boldsymbol{G}$ is weak and in the general case it can be checked (in some cases laboriously) that the dependence does not invalidate any of our conclusions (eg figure 6 for the form of the 'rainbow line').

If the points $\boldsymbol{R}_i$ are sufficiently well separated for the integrand in (3.2) to oscillate many times between them, we may use the method of stationary phase to approximate $S_{\boldsymbol{G}}$. This involves expanding the phase in (3.2) about each point $\boldsymbol{R}_i$ up to terms in $(\boldsymbol{R} - \boldsymbol{R}_i)^2$, and evaluating the resulting Gaussian integrals. We arrive at the following 'simple semiclassical' formula for the diffraction amplitudes:

$$S_{\boldsymbol{G}} \simeq \frac{2\pi}{A(|k_{0z}| + k_z)} \sum_i \gamma_i \frac{\exp\{-i[\boldsymbol{G} \cdot \boldsymbol{R}_i + (|k_{0z}| + k_z)h_p(\boldsymbol{R}_i)]\}}{(|\mathcal{K}(\boldsymbol{R}_i)|)^{1/2}}, \tag{3.5}$$

where the summation is over all points $\boldsymbol{R}_i$ reflecting particles with deviation $\boldsymbol{G}$, and

$$\gamma_i \equiv \begin{cases} +i & \\ -i & \text{if the phase } [\ldots] \text{ in (3.2) has at } \boldsymbol{R}_i \text{ a} \\ 1 & \end{cases} \begin{matrix} \text{minimum} \\ \text{maximum} \\ \text{saddle point,} \end{matrix} \tag{3.6}$$

and where $\mathcal{K}(\boldsymbol{R})$ is the *Hessian* of h_p at $\boldsymbol{R}$, defined by

$$\mathcal{K}(\boldsymbol{R}) \equiv \frac{\partial^2 h_p}{\partial x^2}\frac{\partial^2 h_p}{\partial y^2} - \left(\frac{\partial^2 h_p}{\partial x \partial y}\right)^2. \tag{3.7}$$

For the gently-varying surfaces Σ with which we are concerned, it is helpful to visualize $\mathcal{K}(\boldsymbol{R})$ as the *Gaussian curvature* of Σ at $\boldsymbol{R}$, since this quantity differs from $\mathcal{K}$ only by a

factor $[1 + (\nabla h_p)^2]^{-3/2}$, which in turn differs from unity by only a few per cent. The Gaussian curvature is the product of the two principal curvatures at $\boldsymbol{R}$, and is positive where Σ is concave or convex, and negative where Σ is saddle-shaped.

Experimentally what is observed is $|S_{\boldsymbol{G}}|^2$ (equation (3.1)) and the simple semiclassical result (3.5) shows that this quantity consists of a set of 'steady' terms from each classical path, plus cross terms describing interferences between different classical paths. In the extreme classical limit these interference oscillations (of I as a function of $\boldsymbol{G}$ or $\boldsymbol{K}_0$) are too rapid to be detected, and any experiment would detect only their average, which is zero; in this case (3.5) gives

$$|S_{\boldsymbol{G}}|^2_{\text{classical}} = \frac{4\pi^2}{A^2(|k_{0z}| + k_z)^2} \sum_i \frac{1}{|\mathscr{K}(\boldsymbol{R}_i)|}. \tag{3.8}$$

Thus the Gaussian curvature of Σ at $\boldsymbol{R}_i$ is an inverse measure of the *strength of the contribution* from the path i. This can be seen in a purely classical way as follows: from (3.7) and the specular condition (3.4), it follows that $\mathscr{K}(\boldsymbol{R})$ is proportional to the *Jacobian of the mapping* from 'surface space' $\boldsymbol{R}$ onto 'deflection space' $\boldsymbol{G}$, $\boldsymbol{K}_0$ being kept constant; since in the incident beam particles are uniformly distributed over $\boldsymbol{R}$, this Jacobian $|\mathrm{d}\boldsymbol{G}/\mathrm{d}\boldsymbol{R}|$ is an inverse measure of the density of particles scattered into direction $\boldsymbol{G}$.

For a given $\boldsymbol{K}_0$, the intensity scattered with deflection $\boldsymbol{G}$ will be *infinite* whenever any contributing surface point $\boldsymbol{R}_i(\boldsymbol{G}, \boldsymbol{K}_0)$ lies at a place where $\boldsymbol{K}(\boldsymbol{R})$ vanishes. Now the equation

$$\mathscr{K}(\boldsymbol{R}) = 0 \tag{3.9}$$

defines a *line* $\mathscr{L}$ on the surface; each point $\boldsymbol{R}$ of $\mathscr{L}$ defines an 'image' point $\boldsymbol{G}$ according to (3.4), so that the image of $\mathscr{L}$ is also a line, $\mathscr{C}$, in the deflection space $\boldsymbol{G}$. We call $\mathscr{C}$ the *rainbow line*; any of the (densely distributed) diffraction spots lying near $\mathscr{C}$ will be very intense, so that $\mathscr{C}$ should show up clearly on intensity plots across the $\boldsymbol{G}$ plane. In optical terminology $\mathscr{C}$ is a 'caustic' of the reflected 'rays'—it is the locus of rays for which *angular focusing* occurs. Mathematically, $\mathscr{C}$ is a *singularity* in the mapping from $\boldsymbol{G}$ back to $\boldsymbol{R}$. As we cross $\mathscr{C}$ by varying $\boldsymbol{G}$, then two (or sometimes three) surface points $\boldsymbol{R}_i$ coalesce; thus the simple method of stationary phase leading to (3.5) is not applicable, and $S_{\boldsymbol{G}}$ is actually not infinite but merely large, as we shall discuss in more detail in § 4.

Thus according to classical mechanics the observed scattering should be dominated by the line $\mathscr{C}$ on $\boldsymbol{G}$. What is the form of this rainbow line? To answer this we need first to find the form of the line $\mathscr{L}$ on $\boldsymbol{R}$, defined by (3.9), that generates $\mathscr{C}$. Let the centres of the atoms in the top layer of the solid define the lattice points in $\boldsymbol{R}$. Then the surface Σ, considered as a landscape above the $\boldsymbol{R}$ plane, will have *summits* (full circles on figure 1) at the lattice points, because of the strong repulsive forces that the surface atoms exert on the incoming particles. At the corners of each Wigner–Seitz lattice cell—that is at the point farthest from atoms—Σ will have minima, or *immits* (a terminology introduced by Cayley 1859; see also Maxwell 1870; immits are marked open circles on figure 1). On each side of a lattice cell (broken line in figure 1) there must be a *saddle point* (crosses on figure 1). Let us assume that we are dealing with the simplest case where these are the *only* extrema of Σ; it is always possible to introduce more summits, immits or saddles by introducing more atoms into each unit cell of the surface layer. Figure 1 has been drawn for a rectangular lattice; for non-rectangular lattices the Wigner–Seitz cell would be hexagonal, and each summit would be surrounded by six immits and six saddles.

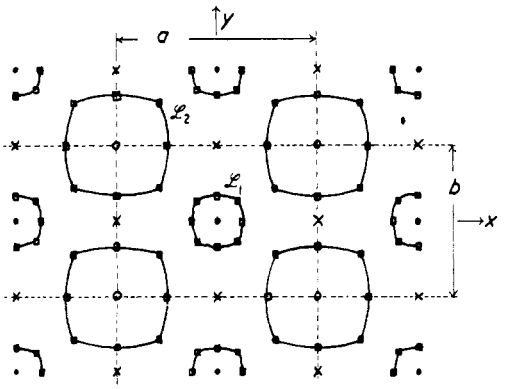

Figure 1. Features of the periodic surface Σ: – – – – – – lattice lines; ● summits; ○ immits; × saddles; —— locus $\mathscr{L}$ of points of zero Gaussian curvature; □ points that must lie on $\mathscr{L}$.

Now the required line $\mathscr{L}$ is the locus of points of zero Gaussian curvature, that is the locus of points where at least one of the two principal curvatures of Σ vanishes. At a summit, both curvatures are (say) negative, at an immit both are positive, at a saddle one curvature is positive and one is negative. Therefore between a saddle and a summit, or a saddle and an immit, we must cross $\mathscr{L}$ $2n-1$ times, where n is an integer; between a summit and an immit both curvatures must change an odd number of times so we must cross $\mathscr{L}$ $2n$ times. The simplest case is $n = 1$, and points satisfying these conditions are marked by open squares on figure 1, and they are joined by a possible line $\mathscr{L}$ (marked full curve). Thus $\mathscr{L}$ consists of closed curves surrounding the regions of positive $\mathscr{K}$ containing summits and immits, while the open region of negative curvature, containing saddles, extends through the lattice. The curves $\mathscr{L}_1$, around summits (figure 1), will generally not have the same shape as the curves $\mathscr{L}_2$, around immits, because summits and immits are not symmetrical features of Σ—they correspond respectively to repulsive regions near atoms and relatively attractive 'interstitial' regions, so that Σ varies more gently near immits than near summits. (Note that it is not possible to satisfy the above conditions on the curvatures if $\mathscr{L}$ surrounds the saddles.)

The rainbow line $\mathscr{C}$ in $\boldsymbol{G}$ is generated from $\mathscr{L}$ by (3.4). The two closed curves $\mathscr{L}_1$ and $\mathscr{L}_2$ (figure 1) will generate two closed curves $\mathscr{C}_1$ and $\mathscr{C}_2$ in $\boldsymbol{G}$. We expect $\mathscr{C}_2$ to lie within $\mathscr{C}_1$, because the slopes $\nabla h_p(\boldsymbol{R})$ of Σ are smaller near immits (ie near $\mathscr{L}_2$) than near summits (ie near $\mathscr{L}_1$). To find the form of $\mathscr{C}_1$ and $\mathscr{C}_2$ we first introduce the special surface

$$h_p^0(\boldsymbol{R}) = h_0\left(\cos\left(\frac{2\pi x}{a}\right) + \cos\left(\frac{2\pi y}{b}\right)\right), \tag{3.10}$$

in which summits and immits are symmetrical. For this form of Σ it is easy to solve (3.10) for $\mathscr{L}$, and we find (as do Garibaldi *et al* 1974) that $\mathscr{L}_1$ and $\mathscr{L}_2$ touch in this special case, and form the following set of intersecting lines across $\boldsymbol{R}$:

$$\begin{aligned} x &= (m+\tfrac{1}{2})a/2 \\ y &= (n+\tfrac{1}{2})b/2 \end{aligned} \tag{3.11}$$

where m and n are integers. Now we use (3.4) and find that the image $\mathscr{C}$ is a single rectangle

given by

$$G_x = \pm \frac{2\pi h_0}{a}(|k_{0z}| + k_z) \qquad \left(|G_y| < \frac{2\pi h_0}{b}(|k_{0z}| + k_z)\right)$$
$$G_y = \pm \frac{2\pi h_0}{b}(|k_{0z}| + k_z) \qquad \left(|G_x| < \frac{2\pi h_0}{a}(|k_{0z}| + k_z)\right). \tag{3.12}$$

In the general case, $h_p(\boldsymbol{R})$ is given not by (3.10) but by

$$h_p(\boldsymbol{R}) = h_p^{(0)}(\boldsymbol{R}) + \epsilon h_p^{(1)}(\boldsymbol{R}), \tag{3.13}$$

where ϵ is a perturbation parameter and $h_p^{(1)}(\boldsymbol{R})$ is any periodic surface not symmetrical in summits and immits. Then our general topological arguments tell us that the rectangular rainbow line (3.12) must split into two as soon as ϵ departs from zero. How does this splitting occur? To answer this we use 'catastrophe theory'; this is a branch of differential topology based on a theorem by Thom (1969, 1972) concerning singularities of mappings defined by gradients (in our case the mapping is $\boldsymbol{G} \to \boldsymbol{R}$, defined by the inverse of (3.4)). The theorem states that the singularities can only be of certain restricted types. In our two-dimensional case the singularities in the plane $\boldsymbol{G}$ are *lines* $\mathscr{C}$, as we know, which are smooth except at isolated points where they may have *cusps*. A cusp is a point where a curve reverses direction as it is traversed; the simplest example of a cusp is the point $x = y = 0$ on the curve $y^2 = x^3$. Thus we expect the rainbow line $\mathscr{C}$ to have cusps. To see how these cusps arise we consider the *rainbow surface* $\mathscr{C}$ generated by adding the third dimension ϵ to the space $\boldsymbol{G}$; this corresponds to looking at all the rainbows from the family of Σ's defined by (3.13). The rainbow surface must have two sheets $\mathscr{C}_1$ and $\mathscr{C}_2$ which touch at $\epsilon = 0$ where it has a rectangular section. Each corner corresponds to a singularity in three dimensions, and the only permitted singularity in which two sheets touch at a corner is, by Thom's theorem, the *hyperbolic umbilic*, illustrated in figure 2. Away from the singularity, that is for nonzero values of ϵ where

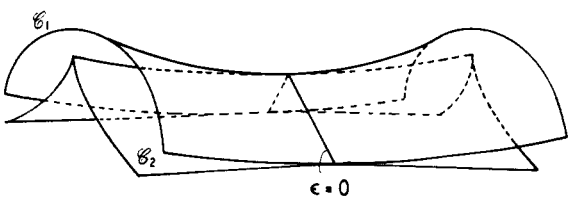

Figure 2. Hyperbolic umbilic catastrophe.

the symmetry of Σ between summits and immits is broken, $\mathscr{C}$ has split into two curves, as expected, and the inner one has a cusp where $h_p^{(0)}(\boldsymbol{R})$ gave a corner. Thus we expect the rainbow lines to take the form shown on figure 3, which is the main result of this section. (For non-rectangular lattices the Wigner–Seitz cell is hexagonal and there would be six cusps.)

These conclusions are supported by a detailed analysis of the special case for which the symmetry-breaking surface modification $h_p^{(1)}(\boldsymbol{R})$ of equation (3.13) is given by

$$h_p^{(1)}(\boldsymbol{R}) = h_0 \cos\left(\frac{2\pi x}{a}\right) \cos\left(\frac{2\pi y}{b}\right); \tag{3.14}$$

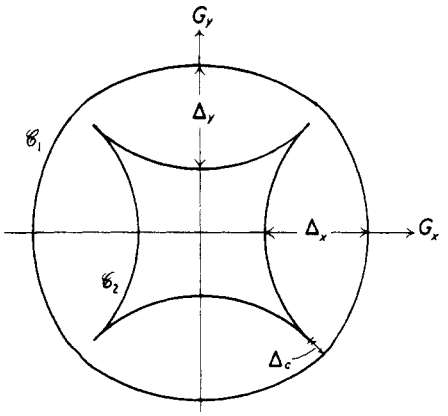

Figure 3. General form of rainbow lines: $\mathscr{C}_1$ and $\mathscr{C}_2$ originate near summits and immits of Σ respectively.

the rainbow lines $\mathscr{C}$ have precisely the form shown on figure 3. In addition we find that the separation Δ_c in the $\boldsymbol{G}$ plane between $\mathscr{C}_1$ and $\mathscr{C}_2$ at a corner (figure 3) is, for small ϵ

$$\Delta_c = 4\pi\left(\frac{1}{a^2}+\frac{1}{b^2}\right)^{1/2}\epsilon^2 h_0(|k_{0z}|+k_z) \sim \frac{16\pi^2\epsilon^2 h_0\sqrt{2}}{a\lambda_0}. \tag{3.15}$$

It is also easy to calculate the separations Δ_x and Δ_y between $\mathscr{C}_1$ and $\mathscr{C}_2$ (figure 3) along the G_x and G_y axes, and we find

$$\begin{aligned}\Delta_x &= \frac{4\pi}{a}\epsilon h_0(|k_{0z}|+k_z) \sim \frac{16\pi^2\epsilon h_0}{a\lambda_0}\\ \Delta_y &= \frac{4\pi}{b}\epsilon h_0(|k_{0z}|+k_z) \sim \frac{16\pi^2\epsilon h_0}{b\lambda_0}.\end{aligned} \tag{3.16}$$

The computations of McClure (1970, 1971) which gave the first theoretical evidence for rainbows in the classical scattering of particles from surfaces, were insufficiently detailed to show the cusp structure clearly. McClure presents intensity maps of the scattering as a function of polar angles θ and ϕ (in our notation, $G_x = k\sin\theta\cos\phi - K_{0x}$, $G_y = k\sin\theta\sin\phi - K_{0y}$). He uses a Monte Carlo procedure which averages over paths emerging in angular 'bins' whose widths are $\Delta\theta = 1^0$ and 3^0, $\Delta\phi = 5^0$. This is a little too coarse, and obscures much of the detail in figure 3; nevertheless, his intensity maps do show 'ridge' and 'tentpole' features, probably corresponding to smooth parts and cusps of the rainbow line. Strictly speaking the ridges and tentpoles should be infinitely high, because the classical rainbow strength is infinite (although integrable!); however the Monte Carlo procedure does not use the formula (3.8) for the contribution from each path but instead calculates directly the Jacobian $|\mathrm{d}(\theta,\phi)/\mathrm{d}\boldsymbol{R}|$, and thus averages over the angular bins. (In McClure's calculations (3.8) would not apply, because he uses a realistic smooth atom–surface potential rather than the mirror Σ.)

The shape of the rainbow line (figure 3) could in principle give detailed information about the surface Σ; this is clear from (3.15) and (3.16), which depend differently on ϵ. In practice the details of $\mathscr{C}$ will be blurred, to a greater or lesser degree by diffraction and by thermal motion of Σ; we consider these effects in more detail in the next two sections.

4. Perfect periodicity: sewing the quantum flesh on the classical bones

There are two kinds of quantum or diffraction effect which conspire to obscure the details of $\mathscr{C}$. The first arises because $\boldsymbol{G}$ is not a continuous variable but consists of reciprocal lattice points; thus patterns in the $\boldsymbol{G}$ plane (eg figure 3) are sampled at discrete points, and these will usually miss the rainbow line. The second is that the function $|S_{\boldsymbol{G}}|^2$ (equation (3.1)) which is sampled is not given precisely by the classical or semiclassical formulae (3.8) or (3.5), which diverge on $\mathscr{C}$, but by the diffraction integral (3.2), which is large but finite on $\mathscr{C}$. Expressing these effects in another way, we can say that interference between waves emerging from different points in the same lattice cell in $\boldsymbol{R}$ blurs out the rainbow line into a diffraction pattern in $\boldsymbol{G}$, while interference between waves emerging from equivalent points in different cells quantizes $\boldsymbol{G}$ so that this diffraction pattern is sampled at discrete points.

First we discuss the blurring of $\mathscr{C}$ by diffraction. Near to a smooth portion of $\mathscr{C}$ the semiclassical formula (3.5) breaks down because two contributing surface points (say $\boldsymbol{R}_1$ and $\boldsymbol{R}_2$) coalesce, thus violating the condition for the applicability of the method of stationary phase. In these circumstances we require a *uniform approximation* to $S_{\boldsymbol{G}}$, that is, a formula for (3.2) which is valid on and near $\mathscr{C}$ and which reduces to (3.5) far from $\mathscr{C}$. Uniform approximations to integrals were invented by Chester *et al* (1957), introduced into scattering theory by Berry (1966) (see also Berry and Mount 1972), and shown to be numerically extremely accurate by Mount (1973).

In the present problem the result is that the contribution $S_{\boldsymbol{G}}^{(\text{rainbow})}$ from $\boldsymbol{R}_1$ and $\boldsymbol{R}_2$ in (3.5) must be replaced by the following formula, involving *Airy functions* Ai (Abramowitz and Stegun 1964) and their derivatives Ai′:

$$S_{\boldsymbol{G}}^{(\text{rainbow})} = \frac{2\pi\sqrt{\pi}\exp[\frac{1}{2}\mathrm{i}(\Phi_1+\Phi_2-\frac{3}{2}\pi)]}{A(|k_{0z}|+k_z)}\left[\left(\frac{1}{\mathscr{K}_1^{1/2}}+\frac{1}{(-\mathscr{K}_2)^{1/2}}\right)\left(\frac{3(\Phi_2-\Phi_1)}{4}\right)^{1/6}\right.$$
$$\times \mathrm{Ai}\,[-(\tfrac{3}{4}(\Phi_2-\Phi_1)^{2/3}]-\mathrm{i}\left(\frac{1}{\mathscr{K}_1^{1/2}}-\frac{1}{(-\mathscr{K}_2)^{1/2}}\right)\left(\frac{4}{3(\Phi_2-\Phi_1)}\right)^{1/6}$$
$$\left.\times \mathrm{Ai}\,'[-(\tfrac{3}{4}(\Phi_2-\Phi_1))^{2/3}]\right]. \tag{4.1}$$

Here Φ denotes the phase

$$\Phi \equiv -[\boldsymbol{G}\cdot\boldsymbol{R}+(|k_{0z}|+k_z)h_{\mathrm{p}}(\boldsymbol{R})] \tag{4.2}$$

in (3.5), and the subscripts 1 and 2 refer to the two contributing points $\boldsymbol{R}_1$ and $\boldsymbol{R}_2$. *On the illuminated side* of the rainbow $\mathscr{C}$ the two Gaussian curvatures $\mathscr{K}_1$ and $\mathscr{K}_2$ will have opposite signs, and we have chosen $\boldsymbol{R}_1$ so that $\mathscr{K}_1$ is positive and assumed that Φ_1 is a minimum. The real positive root of $(\Phi_2-\Phi_1)^{2/3}$ is taken, so that the Airy functions have a negative argument and are thus oscillatory functions (figure 10.6 of Abramowitz and Stegun 1964); equation (4.1) then describes the 'supernumerary rainbows' (Airy 1838, Ford and Wheeler 1959). For deflections $\boldsymbol{G}$ *on the dark side of* $\mathscr{C}$ there are no real paths $\boldsymbol{R}_1$ and $\boldsymbol{R}_2$, and we require complex solutions of (3.4); we can then take a real negative root of $(\Phi_2-\Phi_1)^{2/3}$, and the Airy functions have a positive argument, and decay exponentially 'into the shadow'. On $\mathscr{C}$ the expression (4.1) is finite, and a little analysis shows that $|S_{\boldsymbol{G}}|^2$ rises to a value of order $(h_0/\lambda_0)^{1/3}$ larger than in the 'classical' region away from $\mathscr{C}$ (h_0 is a measure of the maximum excursion of Σ from the $\boldsymbol{R}$ plane). By analysing the special surface (3.10) Garibaldi *et al* (1974) also discuss the diffractive softening of the rainbow singularity; they obtain an expression for $S_{\boldsymbol{G}}^{(\text{rainbow})}$ in terms of Bessel functions

of large order; these can, however, be uniformly approximated by Airy functions (Abramowitz and Stegun 1964) so that the formalism of these authors is a special case of ours.

Near a *cusp* of $\mathscr{C}$, even (4.1) breaks down, because not two but three points $\boldsymbol{R}_i$ coalesce. Instead of Airy functions we must use the following function to describe the diffraction (Pearcey 1946, Berry and Nye 1975):

$$C(X, Y) \equiv \int_{-\infty}^{\infty} \mathrm{d}t \exp\left[\mathrm{i}\left(\frac{t^4}{8} - \frac{t^2 X}{2} + tY\right)\right]. \tag{4.3}$$

The variables X and Y are smooth distortions of G_x and G_y, the manner in which the distortions must be carried out (to obtain a uniform approximation) being explained by Connor (1973). It turns out that on the cusp itself $|S_{\boldsymbol{G}}|^2$ rises to a value of order $(h_0/\lambda_0)^{1/2}$ larger than in the 'classical' region away from $\mathscr{C}$, so that the cusps are the most strongly diffracting parts of the rainbow line. A contour map of $|C(X, Y)|^2$ constitutes figure 4; it is seen how the Airy oscillations appear as we cross $\mathscr{C}$ far from the cusp at $X = Y = 0$.

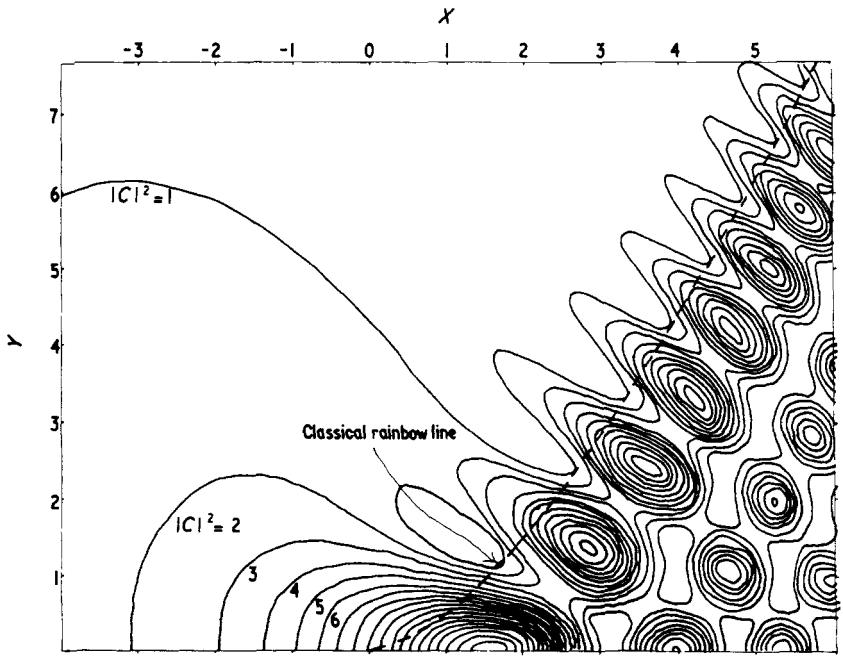

Figure 4. Contours of the cusp diffraction function $|C|^2$ (equation (4.3)).

These results concerning the uniform approximation of the diffraction integral (3.2) are summarized in figure 5.

Now we consider how the visibility of rainbows is affected by the quantization of $\boldsymbol{G}$. The principle is that to observe clearly any feature in the $\boldsymbol{G}$ plane it must be densely covered with diffraction spots. Consider for example, the separation Δ_x between rainbow lines $\mathscr{C}_1$ and $\mathscr{C}_2$ along the G_x axis (figure 3); Δ_x is given by equation (3.16). The G_x spacing

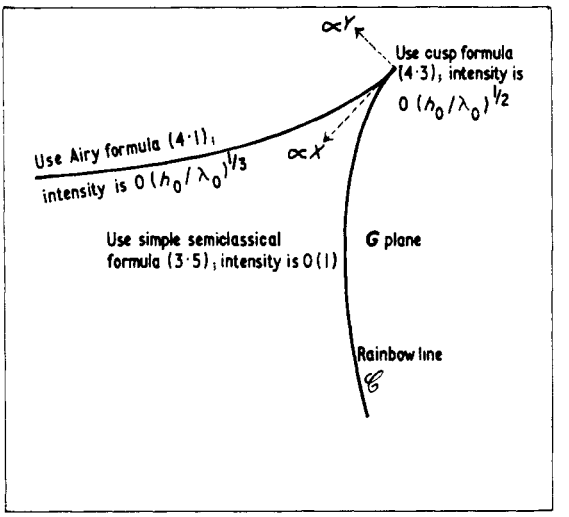

Figure 5. Summary of semiclassical diffraction formulae.

of diffraction spots is $2\pi/a$. Therefore the number $\mathcal{M}_x$ of diffraction spots between $\mathscr{C}_1$ and $\mathscr{C}_2$ is

$$\mathcal{M}_x = 2\epsilon h_0(|k_{0z}| + k_z) \sim \frac{4\pi\epsilon h_0}{\lambda_0}(\cos\theta_0 + \cos\theta), \tag{4.4}$$

where θ_0 and θ are the angles made with the z direction by the incident and scattered particles. For $\mathscr{C}_1$ and $\mathscr{C}_2$ to be distinguishable, $\mathcal{M}_x$ must be large, ie

$$\frac{\lambda_0}{h_0} \ll 4\pi\epsilon(\cos\theta_0 + \cos\theta). \tag{4.5}$$

Another 'feature' is the separation Δ_c between a cusp of $\mathscr{C}_2$ and the nearest 'corner' of $\mathscr{C}_1$ (figure 3); from (3.16), the number $\mathcal{M}_c$ of diffraction spots in Δ_c is

$$\mathcal{M}_c = 2\epsilon^2 h_0(|k_{0z}| + k_z) \sim \frac{4\pi\epsilon^2 h_0}{\lambda_0}(\cos\theta_0 + \cos\theta). \tag{4.6}$$

This must be large, so that we require

$$\frac{\lambda_0}{h_0} \ll 4\pi\epsilon^2(\cos\theta_0 + \cos\theta) \tag{4.7}$$

which is more restrictive than (4.5) if $\epsilon < 1$.

Conditions (4.5) and (4.7) for the distinguishability of two rainbow lines are necessary but not sufficient, because we must also demand that the diffraction spots are sufficiently densely packed for the *individual* rainbow lines to be resolved. A reasonable condition for this is that the number of spots $\mathcal{M}_r$ in the largest Airy-function maximum of equation (4.1) is large. This maximum spans the argument range from about 0 to -2 (Abramowitz and Stegun 1964), so that, from (4.1), we require that the deviation Δ_r in $\boldsymbol{G}$ space from the

rainbow line is such that the difference in phase between the two contributing paths is

$$\Phi_2 - \Phi_1 = \frac{4\sqrt{8}}{3}. \tag{4.8}$$

Since the problem of the width of a single rainbow maximum is essentially one-dimensional, we can confine our attention to the G_x axis, and calculate the width Δ_r by treating h_p as varying only with x, so that the phase Φ in (4.2) depends only on G_x and x. Now x is related to G_x via the path equation (3.4), which now reads

$$\frac{\partial \Phi(G_x, x)}{\partial x} = 0. \tag{4.9}$$

Thus we can write the phase of a path as $\Phi(G_x, x(G_x))$; we wish to expand this function about the rainbow direction G_{xr} for which in addition to (4.9) we must have (3.9), which in one dimension is

$$\frac{\partial^2 \Phi(G_x, x)}{\partial x} = 0. \tag{4.10}$$

The expansion is tricky; for $G_x < G_{xr}$ there are two contributing paths. Their phase difference turns out to be

$$\Phi_2 - \Phi_1 = \frac{4\sqrt{2}}{3}\left|\frac{(\partial^2\Phi(G_{xr}, x_r)/\partial x \partial G_x)^3}{\partial^3 \Phi(G_{xr}, x_r)/\partial x^3}(G_{xr} - G_x)^3\right|^{1/2}, \tag{4.11}$$

where x_r is $x(G_r)$, that is the coordinate for which $h_p(x)$ has a point of inflexion, giving a maximum deviation. Putting in the explicit form (4.2) for Φ and using (4.8) we obtain for the width $\Delta_r = |G_{xr} - G_x|$ the expression

$$\Delta_r = \frac{[4|\mathrm{d}^3 h_p(x_r)/\mathrm{d}x^3| k(\cos\theta_0 + \cos\theta)]^{1/3}}{1 - (\mathrm{d}h_p(x_r)/\mathrm{d}x)\tan\theta}. \tag{4.12}$$

It is not hard to show that the denominator never vanishes. For the cosine surface (3.10) Δ_r becomes

$$\Delta_r = \frac{(2\pi/a)(8\pi(\cos\theta_0 + \cos\theta)h_0/\lambda)^{1/3}}{1 + (2\pi h_0 \tan\theta/a)} \simeq \frac{4\pi}{a}\left(\frac{2\pi h_0}{\lambda_0}\right)^{1/3}. \tag{4.13}$$

For the number $\mathscr{M}_r$ of diffraction spots this gives

$$\mathscr{M}_r = \frac{(8\pi(\cos\theta_0 + \cos\theta)h_0/\lambda)^{1/3}}{1 + (2\pi h_0 \tan\theta/a)} \simeq 2\left(\frac{2\pi h_0}{\lambda_0}\right)^{1/3}. \tag{4.14}$$

In the most favourable case $\theta_0 = \theta = 0$ (ie $\boldsymbol{K}_0 = \boldsymbol{G} = 0$) the criterion for clearly resolving the rainbow structure is

$$\frac{h_0}{\lambda_0} \ll 16\pi. \tag{4.15}$$

In practical cases the value of h_0 might be about 0·5 Å. Then if the incoming particles have $\lambda_0 \sim 0{\cdot}1$ Å, (4.14) gives $\mathscr{M}_r \sim 6$ so that the rainbow structure should be clearly resolved. If in addition the 'asymmetry parameter' ϵ is 0·1, (4.4) gives $\mathscr{M}_x \sim 12$, so that $\mathscr{C}_1$ and $\mathscr{C}_2$ could just be distinguished along the G_x axis of figure 3. However (4.6) gives $\mathscr{M}_c \sim 1$, so that the cusp structure would be confused in this case.

5. Inelastic and diffuse incoherence effects from random perturbations

When a random perturbation $h_r(\boldsymbol{R}, t)$ is added to $h_p(\boldsymbol{R})$, the scattered intensity I is no longer given by the series (3.1) of elastic diffracted beams with quantized directions $\boldsymbol{K} = \boldsymbol{K}_0 + \boldsymbol{G}$. Instead we use the Kirchhoff formalism of § 2; equations (2.5), (2.8) and (3.2) give

$$I(\boldsymbol{K}_0, \omega_0; \boldsymbol{K}, \omega) = \frac{\Sigma_{\boldsymbol{G}_1} \Sigma_{\boldsymbol{G}_2} S_{\boldsymbol{G}_1} S^*_{\boldsymbol{G}_2}}{(2\pi)^3 \mathscr{A}\mathscr{T}} \iint \mathrm{d}\boldsymbol{R}_1 \iint \mathrm{d}\boldsymbol{R}_2 \int \mathrm{d}t_1 \int \mathrm{d}t_2 J$$

where

$$J \equiv \exp\{\mathrm{i}[(\boldsymbol{K}_0 - \boldsymbol{K}) \cdot (\boldsymbol{R}_1 - \boldsymbol{R}_2) - (\omega_0 - \omega)(t_1 - t_2) + \boldsymbol{G}_1 \cdot \boldsymbol{R}_1 - \boldsymbol{G}_2 \cdot \boldsymbol{R}_2 - (|k_{0z}| + k_z)(h_r(\boldsymbol{R}_1, t_1) - h_r(\boldsymbol{R}_2, t_2))]\}. \tag{5.1}$$

Now we must *average* I over the ensemble of random functions $h_r(\boldsymbol{R}, t)$. Because the perturbation of Σ is the summation of a multitude of small independent effects ('surface phonons'), h_r is *Gaussian random* (Rice 1944, 1945, Longuet-Higgins 1956). Denoting ensemble averages by $\langle \cdots \rangle$, we can now use standard noise theory to give, for the average of the function of h_r appearing in (5.1),

$$\langle \exp[-\mathrm{i}(|k_{0z}| + k_z)(h_r(\boldsymbol{R}_1, t_1) - h_r(\boldsymbol{R}_2, t_2))] \rangle = \exp[-H_2(|k_{0z}| + k_z)^2 (1 - C(\boldsymbol{R}_1 - \boldsymbol{R}_2, t_1 - t_2))], \tag{5.2}$$

where H is the RMS value of h_r, namely

$$H = (\langle h_r^2(\boldsymbol{R}, t) \rangle)^{1/2}, \tag{5.3}$$

and C is the autocorrelation function of h_r, namely

$$C(\boldsymbol{R}_1 - \boldsymbol{R}_2, t_1 - t_2) \equiv \frac{\langle h_r(\boldsymbol{R}_1, t_1) h_r(\boldsymbol{R}_2, t_2) \rangle}{\langle h_r^2(\boldsymbol{R}, t) \rangle}. \tag{5.4}$$

The mean value $\langle h_r \rangle$ is zero by definition. Why have we chosen random noise theory for ensemble averaging, rather than a rigorous thermal method based on the density matrix (eg that of Glauber 1955)? For two reasons: first, it is not clear how the co-ordinates and potentials of the surface atoms define the rippling mirror surface Σ; and, second, the crystal structure, and vibratory departures from that structure, are both different at the surface from the bulk (indeed it is the aim of atomic scattering experiments to discover these differences).

Several of the integrations in (5.1) can now be performed, and we get

$$I = \sum_{\boldsymbol{G}} \frac{|S_{\boldsymbol{G}}|^2}{(2\pi)^3} \mathrm{e}^{-H^2 q^2} \iint \mathrm{d}\boldsymbol{R} \int \mathrm{d}t \exp\{\mathrm{i}[(\boldsymbol{K}_0 - \boldsymbol{K} + \boldsymbol{G}) \cdot \boldsymbol{R} - (\omega_0 - \omega)t]\} \mathrm{e}^{H^2 q^2 C(\boldsymbol{R}, t)}, \tag{5.5}$$

where we introduce the notation

$$q \equiv |k_{0z}| + k_z = (k_0^2 - K_0^2)^{1/2} + (k^2 - K^2)^{1/2} = k_0 \cos\theta_0 + k \cos\theta. \tag{5.6}$$

For large values of $\boldsymbol{R}$ or t, C vanishes (there can be no correlation between widely separated events); therefore we separate the 'tail' of the integrals in (5.5) by writing

$$\mathrm{e}^{H^2 q^2 C} = 1 + (\mathrm{e}^{H^2 q^2 C} - 1). \tag{5.7}$$

This gives

$$I(\boldsymbol{K}_0, \omega_0; \boldsymbol{K}, \omega) = \delta(\omega-\omega_0)\sum_{\boldsymbol{G}} |S_{\boldsymbol{G}}|^2 \, \mathrm{e}^{-H^2q^2}\delta(\boldsymbol{K}-\boldsymbol{K}_0+\boldsymbol{G}) + \sum_{\boldsymbol{G}} |S_{\boldsymbol{G}}|^2 I^{\mathrm{r}}(\boldsymbol{K}_0-\boldsymbol{K}+\boldsymbol{G}, \omega-\omega_0), \tag{5.8}$$

where

$$I^{\mathrm{r}}(\boldsymbol{Q}, \Omega) \equiv \frac{\mathrm{e}^{-H^2q^2}}{(2\pi)^3}\iint \mathrm{d}\boldsymbol{R}\int \mathrm{d}t \exp[\mathrm{i}(\boldsymbol{Q}\cdot\boldsymbol{R}-\Omega t)](\mathrm{e}^{H^2q^2C(\boldsymbol{R},t)}-1). \tag{5.9}$$

These results are exact (on our model). They show that the scattered particles emerge in the form of: (*a*) *coherent* elastically diffracted beams whose strengths $|S_{\boldsymbol{G}}|^2$ (cf (3.14)) are reduced by the familiar Debye–Waller factor; and (*b*) *incoherent* fans of radiation whose shape is determined by the correlations of h_{r} by the function I^{r} defined by (5.9). If h_{r} is time-independent (a 'frozen random surface'), then C depends only on $\boldsymbol{R}$ and I^{r} contains the factor $\delta(\Omega)$, so that the diffraction is all elastic and the only effect of incoherence is *diffuse* scattering between the beams at $\boldsymbol{K}_0+\boldsymbol{G}$. If on the other hand h_{r} is space-independent (so that the periodic surface 'shivers' up and down as a rigid whole), then C depends only on t and I^{r} contains the factor $\delta(\boldsymbol{Q})$, so that all diffraction appears in the beams $\boldsymbol{K}_0+\boldsymbol{G}$ and the only effect of incoherence is *inelastic* scattering into frequencies ω different from ω_0.

If $Hq \sim 4\pi H/\lambda$ is small the exponential involving C in (5.9) can be expanded, and I^{r} is easy to evaluate in terms of the phonon spectrum; this is the 'one-phonon case' (Beeby 1972). However, H is of the same order of magnitude as the amplitude of thermal vibrations in the solid, that is, about 0·1 Å; thus, even if λ is as large as 1 Å, Hq exceeds unity and we have to consider 'multiphonon processes'. The novel contribution of this section is an approximation to the integrand of (5.9) that enables I^{r} to be evaluated in simple closed form for any value of Hq. We introduce the 'exponential substitution'

$$\mathrm{e}^{H^2q^2C(\boldsymbol{R},t)}-1 \simeq (\mathrm{e}^{H^2q^2}-1)C\left(\frac{Hq\boldsymbol{R}}{(1-\mathrm{e}^{-H^2q^2})^{1/2}}, \frac{Hqt}{(1-\mathrm{e}^{-H^2q^2})^{1/2}}\right). \tag{5.10}$$

This has remarkable properties (Berry 1973); it is exact when R or t is infinite, and when $\boldsymbol{R}$ and t are zero; it correctly describes the quadratic departure of the left-hand side from $\mathrm{e}^{H^2q^2}-1$ when $\boldsymbol{R}$ or t is small; it is correct for all $\boldsymbol{R}$ and t if Hq is small ('one-phonon case'). Thus for an (unphysical) 'step' correlation function, falling abruptly from unity to zero for one value of $|\boldsymbol{R}|$ and t, (5.10) is exact. For the Gaussian function C, whose 'isotropic' form is

$$C(\boldsymbol{R}, t) = \mathrm{e}^{-R^2/2R_0^2}\,\mathrm{e}^{-t^2/2t_0^2}, \tag{5.11}$$

(5.10) is quite accurate, as figure 6 shows. Where the exponential substitution is poor is when Hq is large and C is negative, but this kind of 'anticorrelation' would only occur if h_{r} were quasi-periodic; however, the dominant periodicity of Σ is already incorporated in $h_{\mathrm{p}}(\boldsymbol{R})$, and negative values for C are unlikely.

Now we can evaluate the incoherence function I^{r}, in terms of the *spectrum* $\bar{C}(\boldsymbol{Q}, \Omega)$ of the correlations of h_{r}; this function is defined as

$$\bar{C}(\boldsymbol{Q}, \Omega) \equiv \frac{1}{(2\pi)^3}\iint \mathrm{d}\boldsymbol{R}\int \mathrm{d}t \exp[\mathrm{i}(\boldsymbol{Q}\cdot\boldsymbol{R}-\Omega t)]C(\boldsymbol{R}, t). \tag{5.12}$$

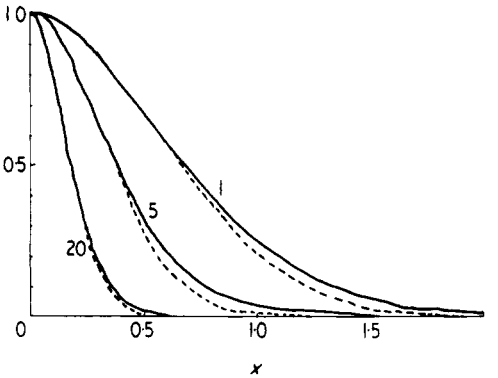

Figure 6. Test of exponential substitution (5.10) for Gaussian autocorrelation function: we plot $(e^{A\exp(-x^2)}-1)/(e^A-1)$ (full lines) and $e^{-Ax^2/(1-e^{-A})}$ (dotted lines) against x for $A = 1$, 5 and 20.

$\bar{C}$ measures the strength of the $\boldsymbol{Q}, \Omega$ Fourier component of $h_r(\boldsymbol{R}, t)$; it can be called the 'surface phonon spectrum'. Using (5.10), (5.9) now becomes

$$I^r(\boldsymbol{Q},\Omega) \simeq \frac{(1-e^{-H^2q^2})^{5/2}}{H^3q^3}\bar{C}\left(\frac{\boldsymbol{Q}(1-e^{-H^2q^2})^{1/2}}{Hq}, \frac{\Omega(1-e^{-H^2q^2})^{1/2}}{Hq}\right). \tag{5.13}$$

This is the main result of this section.

Two limiting cases are of interest. If Hq is small, we can expand the exponentials, and we get

$$I^r(\boldsymbol{Q},\Omega) \xrightarrow{Hq\ \text{small}} H^2q^2\bar{C}(\boldsymbol{Q},\Omega). \tag{5.14}$$

This corresponds to h_r being a weak perturbation of Σ. Almost all the scattering is into the elastic diffracted beams; incoherence effects are small, and the scattering deviating by $\boldsymbol{Q}$ and Ω from an elastic beam comes from the 'surface phonon' with wavevector $\boldsymbol{Q}$ and frequency Ω.

The other limit is large Hq; then the exponentials are negligible and

$$I^r(\boldsymbol{Q},\Omega) \xrightarrow{Hq\ \text{large}} \frac{1}{H^3q^3}\bar{C}\left(\frac{\boldsymbol{Q}}{Hq}, \frac{\Omega}{Hq}\right). \tag{5.15}$$

In this case h_r is so large (in comparison with λ) that even the incoherent scattering is classical. The elastic beams now have negligible intensity, because of the Debye–Waller factor. In this case the scattering into $\boldsymbol{Q}$ and Ω comes not from the 'phonon' with $\boldsymbol{Q}$ and Ω, but from that with wavevector $\boldsymbol{Q}/Hq$ and frequency Ω/Hq. This is understandable classically in terms of the atoms bouncing specularly off the moving phonons: if $\boldsymbol{Q}$ corresponds to a deviation $\Delta\theta = |\boldsymbol{Q}|/k$ from the diffracted beam direction, then

$$\frac{|\boldsymbol{Q}|}{Hq} \sim \frac{k\Delta\theta}{2Hk} = \frac{\Delta\theta}{2H}; \tag{5.16}$$

a 'phonon' with this wavenumber and amplitude H has a maximum slope $\Delta\theta/2$, and so can reflect specularly by $\Delta\theta$. If Ω corresponds to an energy change $\Delta E = \hbar\Omega$ from E_0, then

$$\frac{\Omega}{Hq} \sim \frac{\Delta E\hbar}{2H\hbar \times \text{momentum}} = \frac{\Delta v}{2H}, \tag{5.17}$$

where Δv is the change in speed of the atoms; a 'phonon' with this frequency and amplitude H has a maximum (vertical) speed $\Delta v/2$, and so can change the speed of a reflected particle by Δv.

The general result (5.13) shows that the incoherence function I^r for scattering from a given surface always has the same shape; only the scale changes with Hq. This might explain a puzzle described by Beeby (1973): the incoherent scattering seems to have the 'one-phonon' form, even when 'multiphonon processes' are known to dominate.

Perhaps the most useful property of (5.13) is that it suggests that the blurring in direction and energy of the diffracted beams gives directly the 'surface phonon spectrum' $\bar{C}(\boldsymbol{Q}, \Omega)$ (apart from the scaling factor $Hq(1-e^{-H^2q^2})^{1/2}$ which could be obtained by measuring the diminution $e^{-H^2q^2}$ of the strengths of the diffracted beams). For this to be possible the diffracted beams should not be so broadened that they overlap significantly. We can examine this with the aid of the model autocorrelation function (5.11), for which the 'phonon spectrum' (5.12) is given by

$$\bar{C}(\boldsymbol{Q}, \Omega) = \frac{t_0 R_0^2}{(2\pi)^{3/2}} \exp\left(-\frac{Q^2 R_0^2}{2} - \frac{\Omega^2 t_0^2}{2}\right). \tag{5.18}$$

From (5.13), we have, for the 'breadth' Q_b of the diffuse scattering near each diffracted beam,

$$Q_b = \frac{Hq\sqrt{2}}{R_0(1-e^{-H^2q^2})^{1/2}} \rightarrow \begin{cases} \sqrt{2}/R_0 & Hq \text{ small} \\ \dfrac{Hq\sqrt{2}}{R_0} \sim \dfrac{4\pi H\sqrt{2}}{\lambda_0 R_0} & Hq \text{ large.} \end{cases} \tag{5.19}$$

(Q_b is the '1/e halfwidth' of the $\boldsymbol{Q}$ dependence of I^r.) In order to be able to invert experimental data to find $\bar{C}(\boldsymbol{Q}, \Omega)$, Q_b must be small in comparison with the separation $2\pi/a$ of the diffracted beams.

Finally we recognize that diffuse scattering will blur the rainbow structure arising under semiclassical conditions. To resolve an individual Airy maximum, Q_b must be small compared with Δ_r (equation (4.13)), ie

$$\frac{Ha\sqrt{2}}{R_0 \lambda_0^{2/3} (2\pi h_0)^{1/3}} \ll 1. \tag{5.20}$$

For sufficiently small λ_0 this condition is always violated. To resolve the separation between rainbow lines $\mathscr{C}_1$ and $\mathscr{C}_2$ (figure 3) along G_x, Q_b must be small compared with Δ_x or Δ_y (equation (3.16)), ie

$$\frac{aH\sqrt{2}}{4\pi\epsilon h_0 R_0} \ll 1. \tag{5.21}$$

To resolve the separation between a cusp of $\mathscr{C}_2$ and the nearest part of $\mathscr{C}_1$, Q_b must be small compared with Δ_c (equation (3.15)), ie

$$\frac{H\sqrt{2}}{4\pi\epsilon^2[(1/a^2)+(1/b^2)]^{1/2} h_0 R_0} \ll 1. \tag{5.22}$$

These three conditions assume that the scattering from h_r is nearly classical, so that the 'large Hq' limiting form in (5.19) can be used; if, however, the scattering from h_r is weak, we must use the 'small Hq' form for Q_b.

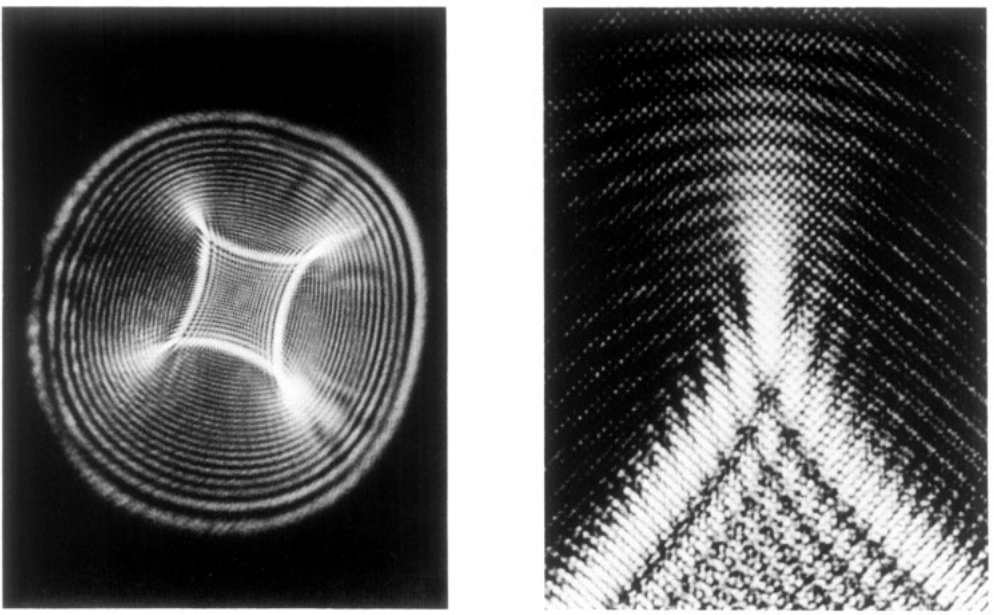

Figure 7. (Plate) (*a*) Caustics of refraction from periodically frosted glass surface ($a = \frac{1}{2}$ mm), using laser light ($\lambda = 6328$ Å). Compare with figures 3 and 4. (*b*) detail near cusp showing quantization into diffraction spots ***G***.

[*facing page* 583]

6. Discussion

The properties of rainbows predicted in §§ 3 and 4 are strikingly confirmed by an optical analogue experiment based on refraction. Laser light transmitted through periodically frosted glass (such as is often used for bathroom windows) is observed on a distant screen. Figure 7(*a*) (plate) is a photograph of the resulting pattern. The two rainbow lines $\mathscr{C}_1$ and $\mathscr{C}_2$ are clearly seen to have the form of figure 3, 'Airy' fringes (equation (4.1)) are clearly seen near smooth parts of $\mathscr{C}$, and diffraction near each cusp of $\mathscr{C}_2$ is clearly of the same form as figure 4; moreover, on a very fine scale (figure 7(*b*) (plate)) it is possible to see the beginning of the quantization of $\boldsymbol{G}$ into diffraction spots, which occurs because the laser beam illuminates several unit cells of the glass surface. Cusped rainbows can also be seen if a distant point source of light is viewed with the eye placed close behind an irregular droplet 'lens' on a glass surface (for example a spectacle lens or car windscreen on a rainy night, or a half-empty wineglass), as explained by Berry and Nye (1975).

In particle scattering from surfaces it would probably not be easy to resolve all the details of the rainbow structure. Thermal diffuse scattering should be minimized by operating at a low temperature, and to see diffraction effects the beam should be as nearly mono-energetic as possible (unless energy-selective detectors are used, so that the 'colours of the rainbow' can be discerned). Finally, the de Broglie wavelength should be as small as possible; this should be achieved with fast light particles rather than heavy particles, to minimize the effects of their impact on the surface. Despite these difficulties, the fine details of surface rainbows ought to be studied experimentally, because they are very sensitive to the details of Σ, as we showed in § 3 (this is generally true of classical effects, the principle being that smaller wavelengths probe finer details).

Now we discuss the method based on equation (5.13) which we suggest might be used to measure the 'phonon spectrum'; of course the theory is not exact: we have used the 'exponential substitution' (5.10), and the rippling-mirror model is itself an approximation, as is the use of Kirchhoff's diffraction integral (2.5). Nevertheless (5.13) should be qualitatively correct for a wide variety of conditions, and at worst would lead to an 'effective surface phonon spectrum' being reconstructed from the experimental measurements.

Acknowledgments

I am happy to thank Professor J P Toennies for the hospitality of the Max-Planck Institüt in Göttingen, Professor H Nahr for introducing me to surface scattering and for several helpful discussions, Professor J A Barker for suggesting the frosted-glass optical analogue and Mr T Osman for making the glass surface used to obtain figure 7 (plate).

References

Abramowitz H and Stegun A 1964 *Handbook of Mathematical Functions* (Washington: US National Bureau of Standards)

Airy G B 1838 *Proc. Camb. Phil. Soc.* **6** 379–402

Beckmann P and Spizzichino A 1963 *The Scattering of Electromagnetic Waves from Rough Surfaces* (Oxford and New York: Pergamon)

Beeby J L 1971 *J. Phys.* C: *Solid St. Phys.* **4** L359–62
—— 1972 *J. Phys.* C: *Solid St. Phys.* **5** 3438–61
—— 1973 *J. Phys.* C: *Solid St. Phys.* **6** 1229–41
Berry M V 1966 *Proc. Phys. Soc.* **89** 479–90
—— 1973 *Phil. Trans. R. Soc.* A **273** 611–58
Berry M V and Mount K E 1972 *Rep. Prog. Phys.* **35** 315–97
Berry M V and Nye J F 1975 to be published
Cabrera N, Celli V, Goodman F O and Manson R 1970 *Surf. Sci.* **19** 67–92
Cayley 1859 *Phil. Mag.* S4 **18** 264–8
Chester C, Friedman B and Ursell F 1957 *Proc. Camb. Phil. Soc.* **53** 599–611
Connor J N L 1973 *Molec. Phys.* **26** 1217–31
Ford K W and Wheeler J A 1959 *Ann. Phys., NY* **7** 259–322
Garibaldi U, Levi A G, Spadacini R and Tommei G E 1974 *Surf. Sci.* to be published
Glauber R J 1955 *Phys. Rev.* **98** 1692–8
Lennard-Jones J E and Devonshire A F 1937 *Proc. R. Soc.* A **158** 253–68
Longuet-Higgins M S 1956 *Phil. Trans. R. Soc.* A **249** 321–87
Maxwell J C 1870 *Phil. Mag.* S4 **40** 421–7 (also in *Collected Works* vol 2)
McClure J D 1970 *J. Chem. Phys.* **52** 2712–8
—— 1971 *J. Chem. Phys.* **57** 2810–22
Mount K E 1973 *J. Phys.* B: *Atom. Molec. Phys.* **6** 1397–411
Pearcey T 1946 *Phil. Mag.* **37** 311–7
Rice S O 1944 *Bell Syst. Tech. J.* **23** 282–332
—— 1945 *Bell Syst. Tech. J.* **24** 46–156
Smith J N Jr, O'Keefe D R, Saltsburg H and Palmer R L 1969 *J. Chem. Phys.* **50** 4667–71
Thom R 1969 *Topology* **8** 313–35
—— 1972 *Stabilité Structurelle et Morphogenèse* (New York: Benjamin)
Toennies J P 1974 *Appl. Phys.* **3** 91–114
Wolken G Jr 1973 *J. Chem. Phys.* **58** 3047–64